THE JOURNAL OF PHYSICAL CHEMISTRY A

Article

Cite This: J. Phys. Chem. A 2018, 122, 9224−9232

pubs.acs.org/JPCA

Barriers for Extrusion of a Guest from the Interior Binding Cavity of a Host: Gas Phase Experimental and Computational Results for Ion-Capped Decamethylcucurbit[5]uril Complexes

Samuel M. Hickenlooper, Conner C. Harper, Brigham L. Pope, Daniel N. Mortensen, and David V. Dearden*

Department of Chemistry and Biochemistry, Brigham Young University, Provo, Utah 84602-5700, United States

ABSTRACT: Factors affecting the extrusion of guests from metal ion-capped decamethylcucurbit[5]uril (mc5) molecular container complexes are investigated using both collision-induced dissociation techniques and molecular mechanics simulations. For guests *without* polar bonds, the extrusion barrier increases with increasing guest volume. This is likely because escape of larger guests requires more displacement of the metal ion caps and, thus, more disruption of the ion-dipole interactions between the ion caps and the electronegative rim oxygens of mc5. However, guests larger than the optimum size for encapsulation displace the ion caps prior to collision-induced dissociation, resulting in less stable complexes and lower dissociation thresholds. The extrusion barriers obtained for guests *with* polar bonds are smaller than those obtained for similarly sized guests *without* polar bonds. This is likely because the partial charges on the guest allow electrostatic interactions with the ion cap and rim oxygens of mc5 during extrusion, thus stabilizing the extrusion transition state and reducing the extrusion barrier. Results from this study demonstrate simple principles to consider for designing host−guest complexes with specific guest-loss behaviors. Similar trends are observed between the experimental and computational results, demonstrating that molecular mechanics simulations can be used to approximate the relative stability of mc5 molecular container complexes and likely those of other similar complexes.

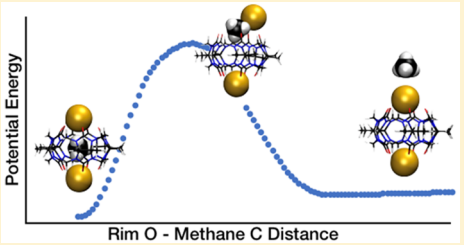

INTRODUCTION

Encapsulation of guest atoms and molecules by supramolecular hosts, or "molecular containers", can be used to generate new structures, such as those used in molecular machines,[1] and to affect the solution-phase[2−4] and gas-phase[5] reactivities of the guests. In solution, solvent and counterion effects can heavily influence the chemistry that occurs between guests and molecular containers. To eliminate these effects and investigate the guest−container relationship directly, molecular container complexes are often investigated in the gas phase,[6] especially in low-pressure environments such as those found in mass spectrometry and ion mobility devices.[5,7−11] A class of molecular containers receiving increased attention for the past two decades is the cucurbit[*n*]uril (CB[*n*]) family.[12] CB[*n*]s are generally produced by condensation of glycoluril in formaldehyde[12,13] and have the structure shown in Figure 1a, with *n* glycoluril subunits. Modifications most commonly occur along the exterior of the container at the locations denoted by "R", although more complex derivatives have also been synthesized.[12,14,15] CB[*n*]s have nonpolar interiors and two openings or "portals" lined with electronegative carbonyl oxygens. CB[*n*]s generally have highly rigid structures, high thermal stabilities, and high binding affinities for certain guests.[12,14,16,17] For example, the binding affinity between CB[7] (Figure 1a, *n* = 7, R = H) and 1,1′-bis(trimethylammoniomethyl)ferrocene (3×10^{15} M^{-1}) is greater than that of the biotin−avidin pair (~1×10^{15} M^{-1}), which has the highest measured binding affinity of any naturally occurring system.[18] The binding affinities between CB[*n*]s and guests depend in part on the size of the guest and the interior volume of the CB[*n*].[5,18]

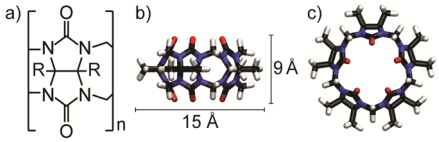

Figure 1. (a) Skeletal formula of a cucurbit[*n*]uril molecule consisting of *n* glycoluril subunits and R groups substituted along the exterior. Graphical representations (tubes) of mc5 from the (b) side and (c) top views. Dimensions of mc5 are taken from ref 53.[55]

CB[*n*]s are commonly complexed with long-chain guests to form supramolecular structures, such as rotaxanes and pseudorotaxanes, and with organic or metal cations, which bind to the rim oxygens of the CB[*n*] portals and function as ionic caps in the resulting supramolecules, encapsulating guests within the interior of the molecular container complexes.[19,20] This type of encapsulation, where guests have only limited electrostatic interactions with the host but are instead sterically trapped by the interactions between the host and the ionic caps, is known as "constrictive binding".[2] Owing to their

Received: August 17, 2018
Revised: November 7, 2018
Published: November 8, 2018

DOI: 10.1021/acs.jpca.8b08031
J. Phys. Chem. A 2018, 122, 9224−9232

resemblance to the selectivity filter in K^+ channels, CB[5] and CB[6] (Figure 1a, n = 5 and 6, respectively, R = H) have also been utilized as alkali metal ion channels in artificial membranes.[21] The relatively small portal and cavity size of CB[5] only allows the transmission of the smallest alkali metal ions (Li^+ and Na^+), whereas the larger portal and cavity size of CB[6] allows the transmission of all of the alkali metal ions.[21] CB[6] has been modified by substituting the locations denoted by "R" with 2-(butylamino)ethanethiol, and the resulting cucurbituril derivative disrupts the cellular membranes in a number of bacterial species.[22] Several CB[n] complexes also traverse cellular membranes,[23] making CB[n]s potentially useful in selective drug delivery.[24−27] CB[n]s have also been utilized for inducing protein dimerization;[28] separating and quantifying sialic acid species;[29] catalyzing oxidation,[30,31] hydrolysis,[32] and ring formation[33] reactions; and altering the photophysical properties of both the ground[34,35] and excited[36,37] states of guests for chemosensing experiments.

The CB[n] investigated in this study is decamethylcucurbit[5]uril (mc5, n = 5, R = CH_3). Graphical representations of mc5 as tubes from the side and top views are shown in Figures 1b and 1c, respectively. Mc5 has an interior volume similar to that of CB[5] (n = 5, R = H), which has an interior volume[12] of 82 Å^3; the two hosts differ only in substituents on their exteriors. Mc5 forms complexes with many cations in solution and selectively binds Pb^{2+}.[38] Gas-phase studies of mc5 indicate that it binds more tightly with small alkali ion caps than with large alkali ion caps and that the binding of a second alkali ion weakens the bond between the first ion cap and mc5 (because of Coulomb repulsion).[39] Trapping bulky guests inside mc5 also affects the binding of the ion caps, with larger guests resulting in weaker binding between the ion caps and mc5.[20]

Here, the extrusion of single-atom and small-molecule guests from mc5 complexes with two alkali metal ion caps is investigated using both collision-induced dissociation techniques and molecular mechanics simulations. Both experimental and computational results indicate that for guests *without* polar bonds the dissociation thresholds for loss of a guest increase with increasing guest volume until the guest becomes large enough to sterically displace the ion caps and thus destabilize the complex. Higher dissociation thresholds are likely obtained with larger guests because escape of larger guests requires more displacement of the metal ion cap than is needed for smaller guests. Lower dissociation thresholds are obtained for guests that have polar bonds than for guests of similar volume that *do not* have polar bonds, likely because the partial charges on the guests interact with the electronegative rim oxygens of mc5 and the positively charged metal ion caps during extrusion. These electrostatic interactions likely stabilize the dissociation transition state structures of these complexes, resulting in lower dissociation thresholds for the loss of guests with polar bonds than for similar guests that do not contain polar bonds. Results from this study demonstrate important principles to consider when designing and developing CB[n] molecular container complexes or similar complexes with specifically desired guest loss properties.

EXPERIMENTAL SECTION

Materials. Mc5 was synthesized at IBC Advanced Technologies (American Fork, UT) using procedures described previously.[38] Argon, acetylene, krypton, and carbon dioxide (in the form of dry ice) were purchased from Airgas (Radnor, PA); xenon from Air Products (Allentown, PA); high purity ammonia from Scott Specialty Gases (Fremont, CA); chloromethane from Sigma-Aldrich (St. Louis, MO); HPLC grade methanol and acetonitrile from Fisher Scientific (Hampton, NH); ethylene-d_4 from Isotech Laboratories (Champaign, IL); potassium acetate, cesium chloride, and ACS grade formic acid from Mallinckrodt (St. Louis, MO); high purity rubidium chloride from MFG Chemical (Dalton, GA); methane from Questar Gas (Salt Lake City, UT); and sodium cyanide from Spectrum Chemical MFG. Corp. (Gardena, CA). All solutions were prepared with an mc5 concentration of 100−200 μM and an alkali salt concentration equal to twice that of mc5. The identity of the alkali salt was varied to obtain the desired ion caps of the mc5 complexes.

Constrictive binding of the guests within the metal-capped mc5 complexes occurs spontaneously in solution. Methanol and acetonitrile were trapped in mc5 complexes by preparing the complexes in 50:50 methanol:water solutions and in neat acetonitrile, respectively. All other host−guest complexes were prepared in 50:50 isopropanol:water solutions (because isopropanol is too large to easily fit within the cavity of mc5, this solvent does not effectively compete with other guest molecules). N_2 and O_2 were trapped spontaneously by exposing the mc5 solutions to air. The CO_2 complex was prepared by adding dry ice to the solution. Other gaseous guests were trapped by heating the solutions to 50 °C to remove dissolved air, sealing and cooling the solutions to room temperature, and then sparging the solution with the gas of interest. Preparation of the xenon complex required the additional step of heating the solution to 50 °C overnight in a septum-capped vial with xenon as headspace gas. A representative mass spectrum of the xenon complex, along with the theoretically predicted mass spectrum for this complex obtained using the mMass software package[40] (http://www.mmass.org), is shown in Figure 2. The peak

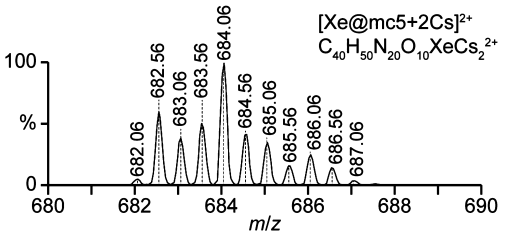

Figure 2. A representative mass spectrum of a guest encapsulated mc5 molecular container complex, Xe trapped inside mc5 with two Cs^+ ion caps ($[Xe@mc5+2Cs]^{2+}$. Dashed lines represent the theoretical specrtum for this complex obtained using the mMass software package.

locations and intensities between the measured and calculated mass spectra are in good agreement, giving us high confidence that we correctly identified the complex. All solutions containing trapped gases were stored in septum-capped vials with the desired guest as headspace gas. All other guest complexes were prepared by adding the guest to the solution at a concentration in excess of that of mc5.

Instrumentation. All experiments were performed using a model APEX 47e Fourier transform ion cyclotron resonance mass spectrometer (Bruker Daltonics, Billerica, MA) equipped with a Midas Predator data system.[41] Ions were generated using a microelectrospray source modified from an Analytica (Branford, MA) design with a metal capillary drying tube

DOI: 10.1021/acs.jpca.8b08031
J. Phys. Chem. A 2018, 122, 9224−9232

based on the design of Eyler.[42] Ions of interest were isolated using stored waveform inverse Fourier transform techniques.[43] Sustained off-resonance irradiation collision-induced dissociation[44] (SORI-CID) experiments were performed on ions of interest by irradiating 1 kHz below resonance for 0.2 s. The total energy deposited into the ions was controlled by varying the peak-to-peak excitation amplitude between 0 and ~8.5 V. Argon collision gas was introduced into the cell at a constant pressure of ~2×10^{-5} mbar using a Freiser-type pulsed leak valve.[45]

Data were analyzed using the Igor Pro software package (version 6, Wavemetrics; Lake Oswego, OR) to extract mass spectral peak amplitudes as a function of the peak-to-peak excitation voltage. The average energy deposited in the ions during SORI-CID (E_{SORI}) is proportional to the cube of the peak-to-peak excitation voltage[46] (V_{pp}) as described in eq 1:

$$E_{SORI} \propto N^* \sigma t_{SORI} \left(\frac{m_{neut}}{m_{neut} + m_{ion}} \right) \frac{V_{pp}^{\ 3}}{m_{ion}^{\ 2}} \quad (1)$$

where N^* is the number density of the neutral collision gas, σ is the collision cross section of the ion, t_{SORI} is the duration of the SORI excitation event, and m_{neut} and m_{ion} are the masses of the neutral collision gas and ion, respectively. Because of the proportionality in eq 1, it is not possible to determine absolute dissociation thresholds using the SORI method, although relative threshold energies can be compared qualitatively. Differences in collision cross sections between the different mc5 complexes were assumed to be negligible. Relative E_{SORI} values corresponding to 50% dissociation of the mc5 complexes ($E_{SORI,50\%}$) were obtained from sigmoidal fits to the survival yields of the complexes as a function of SORI energy (Figure 3a). Reported uncertainties are standard deviations determined from three or more replicate measurements.

Computational Modeling. Molecular mechanics simulations were performed with the Spartan '14 software package (Wavefunction, Inc.; Irvine, CA) using the Merck Molecular Force Field supplied with the program (MMFF94)[47−51] supplemented by van der Waals parameters for Rb^+, Cs^+, Ar, Kr, and Xe, which are developed by analogy to similar species (Table 1). Extrusion barriers were calculated with the "Energy Profile" module by systematically varying the distance between one or more carbonyl oxygen atoms in one rim of mc5 and one of the atoms in the guest with full relaxation of all other atoms and the "CONVERGE" option selected. Reported dissociation barriers are the differences between the lowest energy structures of the guest-trapped complexes and the highest energy intermediate structures found as egress occurs (Figure 3b). Multiple modes of egress were examined, and the reported barriers are the minimum values found for each guest. The volumes of Ar, Kr, and Xe were calculated from their van der Waals radii (1.88, 2.02, and 2.16 Å, respectively),[52] and the volumes and polar surface areas of all other guests were calculated using Spartan '14.

RESULTS AND DISCUSSION

Molecular Mechanics Modeling. The computed potential energy profiles for all of the systems examined share some common features and give insight into the process of guest extrusion from the interior of the complex. In all cases, placement of the guest in the interior of the host is a minimum on the potential energy surface, although at the molecular

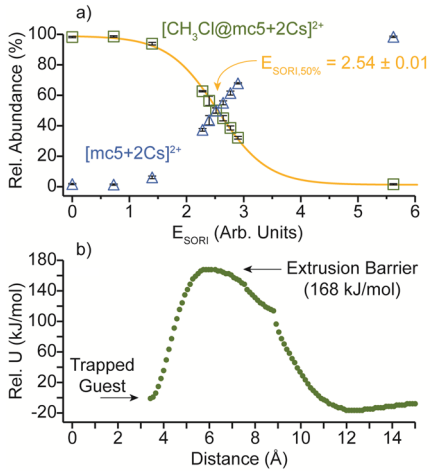

Figure 3. (a) A representative plot of the relative abundance of an mc5 molecular container complex, chloromethane trapped inside mc5 with two Cs^+ ion caps ($[CH_3Cl@mc5+2Cs]^{2+}$, green squares), as a function of SORI energy. The complex dissociates via loss of chloromethane, resulting in empty mc5 with two Cs^+ ion caps ($[mc5+2Cs]^{2+}$, blue triangles). The yellow line denotes a sigmoidal fit to the data obtained for the $[CH_3Cl@mc5+2Cs]^{2+}$ complex. (b) Calculated potential energies for the complex $[CH_3Cl@mc5+2Cs]^{2+}$ as a function of the distance between the carbon atom in chloromethane and the rim oxygens of mc5 initially nearest to the carbon atom (the chlorine atom in chloromethane extrudes first). These potential energies are scaled relative to that of the lowest energy structure of the chloromethane inclusion complex.

Table 1. Supplemental van der Waals Parameters for Select Guests Developed for Molecular Mechanics Simulations by Analogy to Similar Species

symbol	type	Alpha-i	N-i	A-i	G-i	development method
Rb^+	210	1.15	6.5	4	1.3	comparison with K^+
Cs^+	211	1.59	8	4	1.3	fitted from polarizability
Ar	217	0.9	4.5	4	1.3	midway between Ne and Kr
Kr	216	1.45	5.5	4	1.3	iterated to match experiment
Xe	215	2.3	7.5	4	1.4	iterated to match experiment

mechanics level of theory this is not always the global minimum, particularly for guests that have polar bonds. For example, in Figure 3b a structure is obtained after extrusion occurs (distance = 12.2 Å) that is ~16.5 kJ/mol lower in energy (at the MMFF level of theory) than the internally bound complex (distance = 3.4 Å). In contrast, calculations performed at higher levels of theory (M06-2X/6-31+G* calculations with the LANL2DZ basis set for Cs atoms) indicate that interior binding is energetically preferred by at least 9 kJ mol^{-1} even for bulky, polar guests (and by ~40−50 kJ mol^{-1} for guests that better fit the binding cavity). In addition, it is unlikely that the size and shape dependences observed in the experimental results would occur if the guests were externally bound. Thus, we believe that the lower energy structure obtained for the externally bound complex reflects imperfections in the MMFF model rather than the true relative energetics of these different structures.

Points of maximum energy found in the process of extruding the guest, which approximate the transition states for extrusion, always involve displacement of the capping metal cation away from its equilibrium position (optimally bound to the carbonyl oxygens of the mc5 rim) enough to allow egress of the guest.

DOI: 10.1021/acs.jpca.8b08031
J. Phys. Chem. A 2018, 122, 9224−9232

As the guest—rim oxygen distance increases beyond this point in the simulation, the rim cation frequently moves back into binding position perched on the mc5 host within a few more calculation steps, resulting in much lower energy and often an apparent discontinuity in the potential energy plots. One such discontinuity is visible in Figure 3b (distance = 9 Å). This reflects some inadequacy in our use of guest—rim oxygen distance to approximate the extrusion reaction coordinate, but because the discontinuities always occur at distances beyond the maximum energy point and because of the relatively good qualitative agreement between experiment and the model calculations, we feel comfortable in using this computational method to estimate extrusion barriers.

Qualitatively, the extrusion barrier energies extracted from the MMFF modeling show surprisingly good agreement with the measured $E_{SORI,50\%}$ values (Figure 4). With a few

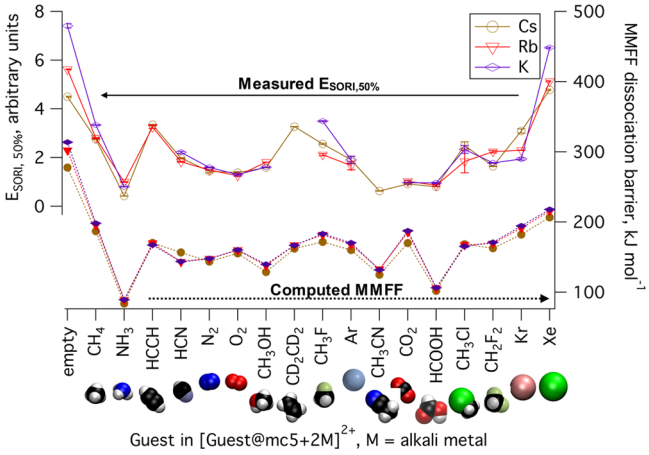

Figure 4. Comparison of experimentally measured $E_{SORI,50\%}$ values (left axis, open shapes) with extrusion barriers (right axis, closed shapes) from MMFF calculations for $[Guest@mc5+2M]^{2+}$ complexes, where M is the ion cap listed in the inset. Guests are listed in order of molecular weight. Note the general qualitative agreement in the two sets of data.

exceptions (notably CO_2, addressed below), guests that have relatively high $E_{SORI,50\%}$ values (such as methane, ethene, ethyne, and xenon) also exhibit relatively high extrusion barriers, and guests that have low $E_{SORI,50\%}$ values (such as ammonia, methanol, formic acid, and acetonitrile) are found by the MMFF calculations to be extruded at relatively low energies. Similarly, the MMFF barrier calculations suggest that in general extrusion energies are slightly lower for Cs^+-capped complexes than for Rb^+-capped complexes, which have slightly lower barriers than K^+-capped complexes. The same general trend is seen in the experimental $E_{SORI,50\%}$ data. Thus, even this extremely inexpensive level of theory is capable of qualitatively predicting the experimental results.

Extrusion of Guests That *Do Not Have* Polar Bonds. The dissociation thresholds of mc5 complexes with two Cs^+ ion caps and various guests that do not have polar bonds, measured using SORI-CID and calculated using molecular mechanics simulations, are shown as a function of the volume of the guest in Figures 4a and 4b, respectively. All of the mc5 host–guest complexes, with the exception of the xenon complex, dissociate via loss of the guest (without loss of a metal ion), likely via a temporary displacement of one of the metal ion caps (Scheme 1). Experimentally, loss of xenon is

Scheme 1. Extrusion of Kr (Green Spheres) from Mc5 with Two Cs^+ Ion Caps (Gray Spheres)

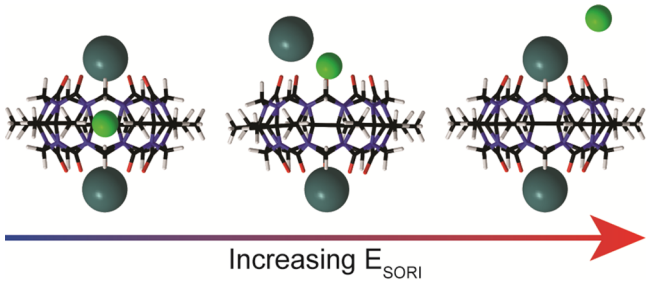

typically accompanied by loss of one of the Cs^+ ion caps. Therefore, the $E_{SORI,50\%}$ values determined for loss of all of the guests but xenon correspond to the extrusion barrier for removing the guests from the complexes.

Both the experimental (Figure 5a) and computational (Figure 5b) results indicate that there is a strong linear

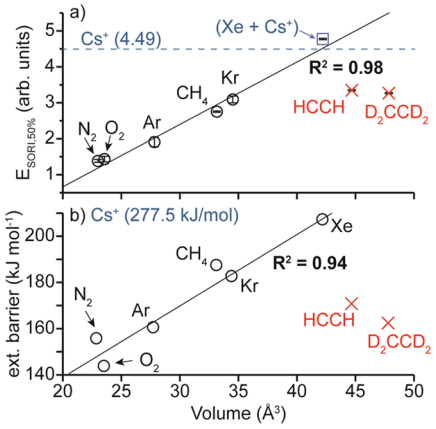

Figure 5. (a) Relative $E_{SORI,50\%}$ values and (b) calculated extrusion barriers for mc5 complexes with guests that do not contain polar bonds and two Cs^+ ion caps as a function of guest volume. Black lines are linear fits to the data excluding that obtained for acetylene (HCCH) and ethylene (D_2CCD_2), which are denoted by red crosses. The blue square in (a) indicates the $E_{SORI,50\%}$ value for loss of xenon and one of the Cs^+ ion caps (included in the linear fit). The relative $E_{SORI,50\%}$ value for loss of one of the Cs^+ ion caps from an empty mc5 complex with two Cs^+ ion caps is indicated in (a) as blue text in parentheses and as a blue dashed line. The calculated dissociation threshold for loss of Cs^+ from such a complex is substantially off scale and is therefore only indicated in (b) as blue text in parentheses.

correlation ($R^2 \geq 0.94$) between the calculated volume of the guest and the dissociation threshold of the complex for all but the largest guests (acetylene and ethylene). The similar trends observed in the experimental and computational results suggest that molecular mechanics simulations using the MMFF94 force field can be used to approximate the relative dissociation thresholds for loss of guests that do not have polar bonds from mc5 complexes. It should be noted, however, that the molecular mechanics simulations predicted loss of xenon from the mc5 complex without loss of an ion cap, whereas loss of xenon and the ion cap occurred simultaneously in all SORI-CID experiments involving Cs^+ caps and is the dominant dissociation pathway when Rb^+ is the capping cation. Unsurprisingly, given the low level of theory, these results suggest our molecular mechanics simulations do not accurately

DOI: 10.1021/acs.jpca.8b08031
J. Phys. Chem. A 2018, 122, 9224–9232

distinguish differences in the dissociation thresholds between loss of a guest and loss of an ion cap.

It is unlikely that the differences in the extrusion barriers of the nonpolar guests arise from host−guest binding energies; rather, larger extrusion barriers are likely obtained with increasing guest volume because smaller guests require less displacement of the metal ion caps to escape than larger guests. Displacement of the ion cap disrupts the ion-dipole interactions between the cap and the electronegative rim oxygens of mc5. Less displacement results in less disruption of the ion-dipole interactions and thus a lower extrusion barrier for smaller guests. The interior of mc5 (Figure 1a) is predominantly nonpolar. Therefore, guests that have no polar bonds experience primarily dispersion interactions with the host within the cavity of mc5. The strength of these interactions is significantly less than that of the ion-dipole interactions between the ion caps and the rim oxygens of mc5. Therefore, we expect the dispersion interactions that occur between the guests and the cavity of mc5 to have negligible effects on the measured dissociation thresholds for the complexes.

The experimental (Figure 5a) and computational (Figure 5b) results obtained for both acetylene and ethylene deviate significantly from the linear relationship observed between guest size and dissociation threshold observed for the other guests without polar bonds. One possible explanation lies in the shapes of these guests. Acetylene and ethylene have long, narrow structures, and less displacement of the metal ion caps might be required to extrude oblong guests than to extrude spherical guests of the same volume. The relatively large size of the acetylene and ethylene guests also likely results in some displacement of the metal ion caps in the mc5 complexes prior to SORI-CID. Support for this interpretation comes from the MMFF modeling, as shown in Table 3. In the model structures, these guests result in significantly greater metal−metal distances than are observed when no guest is present. Displacement of the ion caps should result in weaker ion-dipole interactions between the ion caps and the rim oxygens of mc5 in complexes with oversized guests, and weaker ion-dipole interactions should result in the ion caps being displaced more readily during SORI-CID. In summation, for guests that have no polar bonds, the volume correlates with the extrusion barrier if the guest is roughly spherical. For guests with different shapes, both the volume and shape of the guest affect extrusion, with "long" guests that displace the metal ions having lower extrusion barriers. These results are consistent with previous results indicating that trapping larger guests results in more rapid removal of ion caps from mc5 complexes when reacted with gaseous crown ethers, which was attributed to the larger guests disrupting the binding between the ion caps and mc5.[20]

Table 2. $E_{SORI,50\%}$ Values for Egress of Guests with No Polar Bonds from Doubly Charged Mc5 Complexes with the Indicated Alkali Metals as Caps, Listed in Order of Increasing Guest Volume

		caps		
guest	volume (Å^3)	CsCs	RbRb	KK
O_2	23.0	1.38 ± 0.04	1.25 ± 0.02	1.30 ± 0.03
N_2	23.6	1.43 ± 0.06	1.49 ± 0.01	1.59 ± 0.02
Ar	27.8	1.91 ± 0.14	1.67 ± 0.18	1.90 ± 0.16
CH_4	33.2	2.75 ± 0.01	2.80 ± 0.02	3.33 ± 0.01
Kr	34.5	3.09 ± 0.09	2.30 ± 0.01	1.94 ± 0.04
Xe	42.2	4.77 ± 0.03	5.13 ± 0.03	6.51 ± 0.03
HCCH	44.7	3.35 ± 0.01	3.25 ± 0.05	
CD_2CD_2	47.9	3.27 ± 0.01		

Extrusion of Guests That *Have* Polar Bonds. Relative $E_{SORI,50\%}$ values obtained for mc5 complexes with guests with polar bonds and two Cs^+ ion caps are shown as a function of guest volume in Figure 6a. The correlation between guest volume and dissociation threshold for these guests is very poor (R^2 = 0.06). However, all of the $E_{SORI,50\%}$ values are at least 40% less than those predicated by the linear fit between guest volume and dissociation threshold obtained for the guests that have no polar bonds in Figure 5a. This indicates that the extrusion barrier for loss of a guest with polar bonds is less than that for loss of a guest of the same size *without* polar bonds. We suggest that this is because the presence of partial charges within a guest molecule allows for electrostatic interactions between the guest and the positively charged metal ion caps and the electronegative rim oxygens of mc5 during extrusion. According to both the computational models and the experimental results, all of these complexes dissociate via loss of the guest. As the guest is lost, re-formation of the ion-dipole interactions between the ion cap and the rim oxygens of mc5 is energetically preferable to the loss of the ion cap and retention of the electrostatic interactions between the guest and mc5. However, we believe that the electrostatic interactions between the guest and the rest of the complex stabilize the transition state for extrusion, resulting in lower extrusion barriers for these complexes.

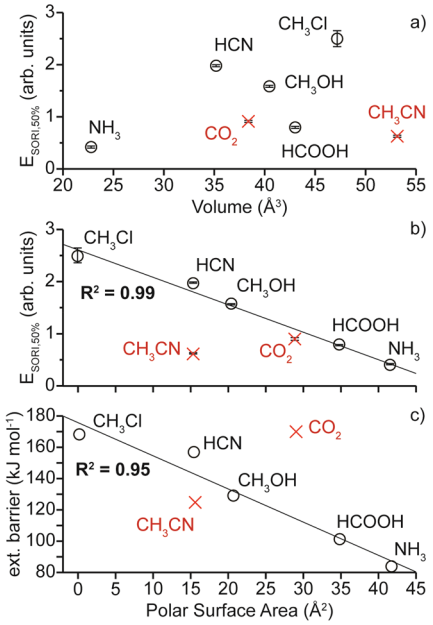

Figure 6. Relative $E_{SORI,50\%}$ values for mc5 complexes with guests with polar bonds and two Cs^+ ion caps as a function of (a) guest volume and (b) guest polar surface area. (c) Calculated extrusion barriers for loss of guests with polar bonds from mc5 complexes with two Cs^+ ion caps as a function of the polar surface area of the guest. Black lines in (b) and (c) are linear fits to the data excluding that obtained for CH_3CN and CO_2 (denoted by red crosses).

One way of quantifying the propensity of a molecule to undergo electrostatic interactions is by calculating the polar

DOI: 10.1021/acs.jpca.8b08031
J. Phys. Chem. A 2018, 122, 9224−9232

surface area of the molecule,[53] which is the sum of the surface area over all oxygen and nitrogen atoms and all hydrogen atoms bonded to oxygen and nitrogen atoms in a molecule. With the exception of acetonitrile and carbon dioxide, both the experimental (Figure 6b) and computational (Figure 6c) results indicate that there is a strong linear correlation ($R^2 \geq 0.95$) between the dissociation threshold and the polar surface area for guests with polar bonds. These results indicate that for guests with polar subgroups the extrusion barrier decreases as the ability of the guest to form noncovalent interactions with the ion cap and rim oxygens of mc5 increases. These results are consistent with a previous study, in which significantly higher rates were reported for both egress from and ingress into the interior of CB[6] in solution for the more electrostatically active protonated form of cyclohexylmethylamine than for the less electrostatically active deprotonated form of this guest.[54] The different rates of ingress and egress reported in that study for the different forms of cyclohexylmethylamine suggest that both the dissociation and association thresholds for CB[6] complexes decrease as the electrostatic activity of the guest increases. The permeation of molecules through many biological membranes also decrease as the polar surface area of a molecule increases.[53] Therefore, we speculate that the results in Figure 6 and those reported by others[54] for CB[6] complexes with the different forms of cyclohexylmethylamine support the suggestion made previously[21] that cucurbit[*n*]urils may be suitable for modeling ion transport through cellular membranes and other biological surfaces. However, it should be noted that the results in Figure 6 were obtained from gas-phase measurements, wherein any interactions between the solvent and membrane that may affect permeation are absent.

The experimental results obtained for CO_2 agree well with this conclusion (Figure 6b), but the extrusion barrier calculated for CO_2 using molecular mechanics simulations (170 kJ mol^{-1}) is ~49% greater than that predicted by the linear fit between extrusion barrier and polar surface area obtained for the other guests with polar bonds. The reason for this disagreement is unclear, but the most tempting explanation is that the MMFF model we used for CO_2 was inadequate. One bit of evidence supporting this notion is that the O−O distance in the MMFF CO_2 (2.352 Å) is somewhat longer than the value calculated at the MP2/6-311+G-(2DF,2P) level of theory (2.335 Å). If the MMFF model does not correctly describe the charge distribution in the CO_2 guest, it might also fail to correctly describe electrostatic interactions between the guest and the capping cations and, thus, yield an excessively large extrusion barrier. The other outlier in these data (acetonitrile) is the guest with the largest volume (53.1 Å^3) and which has a long, mostly linear structure. The lower than expected $E_{SORI,50\%}$ value measured for this guest is likely due to the large size of acetonitrile, which results in a large displacement of the ion caps (Table 3) and a destabilization of the molecular container complex prior to SORI-CID. This is consistent with the results obtained for the relatively large guests that *do not* have polar bonds (acetylene and ethylene).

Effects of Ion Cap Type. The effects of the ion caps on the dissociation threshold for loss of a guest are investigated by measuring the $E_{SORI,50\%}$ values of mc5 complexes with K^+, Rb^+, and Cs^+ ions functioning as caps. Generally, both the MMFF calculations and the experiments show that the effects of the capping cations are small and that extrusion barriers are in the order $K^+ > Rb^+ > Cs^+$, with a few notable exceptions. The ethylene guest complexes with K^+ and Rb^+ ion caps and the acetylene guest complex with K^+ ion caps were not observed to an appreciable extent. For krypton and chloromethane, the largest guests observed in mc5 complexes with the K^+ and Rb^+ ion caps (other than Xe, which is discussed in greater detail below), the $E_{SORI,50\%}$ values follow trends quite different from the usual pattern: they are on average ~24% *less* with the K^+ and Rb^+ ion caps than with the Cs^+ ion caps (Figure 7a). The

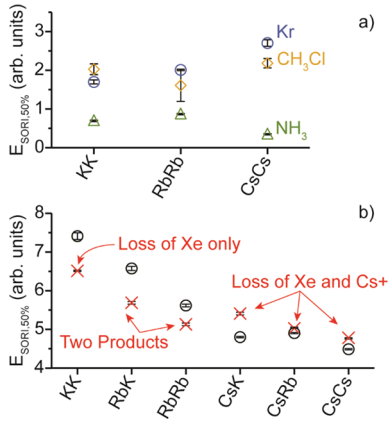

Figure 7. Relative $E_{SORI,50\%}$ values for the dissociation of (a) the guest from mc5 complexes containing krypton (blue circles), chloromethane (yellow diamonds), and ammonia (green triangles) and (b) mc5 complexes containing either no guest (black circles) or xenon (red crosses) as a function of the identity of the metal ion caps.

inability to form complexes with the largest guests (ethylene and acetylene) and the smaller $E_{SORI,50\%}$ values obtained for krypton and chloromethane likely result from the smaller ion caps binding further into the cavity of mc5 than the larger caps,[39] resulting in a decrease in the available volume for trapping guests. This diminished trapping volume is likely too small to accommodate either ethylene or acetylene and likely results in krypton and chloromethane coming into contact with the smaller ion caps, resulting in a displacement of the caps and destabilization of the complexes. This explanation is qualitatively consistent with the computational results of Table 3, which show that displacement of the capping cations by the guest decreases in the order $K^+ > Rb^+ > Cs^+$ for most guests.

It is also interesting to note that the $E_{SORI,50\%}$ value obtained for CH_4 with the K^+ ion caps is ~20% higher than that obtained with the Rb^+ and Cs^+ ion caps. These results are also reflected to some extent in the computational results, wherein higher extrusion barriers are obtained with both the K^+ (198 kJ mol^{-1}) and Rb^+ (196 kJ mol^{-1}) caps than with the Cs^+ (187 kJ mol^{-1}) caps, despite the slightly increased lid displacement required for the K^+ (0.05 Å) and Rb^+ (0.04 Å) caps than for the Cs^+ (0.02 Å) caps. Both the experimental and computational results indicate a higher dissociation threshold is obtained with the smaller ion caps, though the two methods disagree as to whether the higher dissociation threshold is initially obtained with the Rb^+ caps or the K^+ caps. The increased dissociation barrier obtained with the smaller caps might arise simply because the smaller cations are stronger polarizers and therefore bind more strongly. In addition, a tempting explanation is that the decreased interior volume obtained with the smaller caps results in a more optimal binding environment for the mid-sized methane guest.

DOI: 10.1021/acs.jpca.8b08031
J. Phys. Chem. A 2018, 122, 9224−9232

Table 3. Change in Distance between Capping Metal Cations in Decamethylcucurbit[5]uril Complexes Relative to That with No Guest Present, from MMFF Minimum-Energy Geometries for Trapped Guests[a]

		Change in Lid-Lid Distance from Empty Complex, Å		
	Guest	ΔKK	ΔRbRb	ΔCsCs
no Polar Bonds	N_2	0.05	0.04	0.03
	O_2	0.07	0.06	0.04
	Ar	0.01	0.00	0.00
	CH_4	0.05	0.04	0.02
	Kr	0.03	0.01	0.01
	Xe	0.07	0.05	0.02
	HCCH	0.44	0.44	0.43
	D_2CCD_2	0.15	0.11	0.04
Polar Bonds	NH_3	-0.21	-0.21	-0.19
	HCN	0.11	0.08	0.10
	CO_2	0.16	0.12	0.04
	CH_3OH	-0.07	-0.09	-0.11
	HCOOH	0.19	0.17	0.13
	CH_3Cl	0.45	0.40	0.30
	CH_3CN	0.54	0.48	0.40

[a]Distances less than in the "empty" complexes are in red, and distances more than 0.1 Å greater than in the empty complexes are in green.

The $E_{SORI,50\%}$ values for loss of ammonia (Figure 7a) are also significantly higher with the K^+ (0.80 ± 0.01) and Rb^+ (0.99 ± 0.02) ion caps than with the Cs^+ ion caps (0.42 ± 0.00). Ammonia is a relatively small guest but has the highest polar surface area (42.5 $Å^2$) of any guest in this study. Higher extrusion barriers may be obtained for ammonia with the smaller ion caps because smaller ion caps bind more strongly with mc5 than larger ion caps,[39] and this increased binding strength may reduce the relative stability of the dissociation intermediates for loss of ammonia. The smaller cations are also more effective polarizers than the relatively large Cs^+ ion. Ammonia is highly polarizable and therefore may bind more tightly to the smaller, more effective polarizing ions than to the Cs^+ ion, resulting in higher dissociation thresholds for the smaller caps. The $E_{SORI,50\%}$ value obtained for ammonia with the Rb^+ ion caps (0.99 ± 0.02) is slightly larger than that obtained with the smaller K^+ ion caps (0.80 ± 0.01), possibly because the smaller K^+ ions block the mc5 portal slightly less effectively than the larger Rb^+ ions. The $E_{SORI,50\%}$ values for loss of all of the other guests investigated here change by less than 15% as the ion caps are varied (Figure 4; Tables 2 and 4 for guests without and with polar bonds, respectively). These results suggest that for relatively small guests and for guests with relatively low polar surface areas the nature of the ion caps has little impact on the extrusion barrier for loss of a guest.

The effects of the ion caps on the measured $E_{SORI,50\%}$ values for the dissociation of empty mc5 complexes as well as for the dissociation of xenon inclusion mc5 complexes were also investigated with K^+, Rb^+, and Cs^+ caps, including mixed combinations of these caps (Figure 7b). Dissociation of the empty complexes proceeds exclusively via loss of the larger ion cap. This is because smaller ion caps bind more strongly with mc5 than larger caps.[39] The xenon inclusion complexes with one or more Cs^+ caps dissociate via concomitant loss of xenon and Cs^+. In contrast, the Xe inclusion complexes with two Rb^+ caps and the "mixed" complex with one Rb^+ cap and one K^+ cap dissociate via two channels, namely concomitant loss of xenon and Rb^+ and loss of xenon without loss of either cap. The prior pathway occurs at about twice the rate of the latter for both complexes. The inclusion complex with two K^+ caps dissociates exclusively via loss of xenon without loss of either cap. Thus, the retention of both ion caps becomes more favorable as the size of the larger cap decreases, likely because the smaller caps bind more tightly to mc5 than the larger caps, consistent with the results obtained for the empty mc5 complexes.

It is interesting to note that the dissociation thresholds for the Xe−mc5 complexes containing one or more Cs^+ caps are equal to or greater than the dissociation thresholds for the empty complex, whereas the Xe complexes with other metal caps, which can dissociate through loss of the Xe without loss of the cation, have thresholds lower than those for loss of the metal ion from the empty complexes. This is consistent with the expectation that removal of the metal ion combined with extrusion of the guest should require more energy than simply extruding the guest without loss of the metal. In the latter case some of the cost of displacing the metal is recovered as the metal moves back into the binding site, whereas when the metal is lost along with the Xe atom this recovery of energy does not happen.

Finally, it is worth noting that in the mixed-metal Xe complexes that exhibit loss of metal along with loss of Xe, it is always the larger metal cation that is lost along with the Xe atom. This is consistent with our molecular mechanics modeling, which suggests that egress on the side of the larger metal is a lower energy process than egress on the small metal side. While the modeling suggests egress on the large metal side is lower in energy for all guests, the Xe complexes are the only ones where we can observe some experimental verification

Table 4. $E_{SORI,50\%}$ Values for Egress of Guests with Polar Bonds from Doubly Charged Mc5 Complexes with the Indicated Alkali Metals as Caps, Listed in Order of Increasing Polar Surface Area of the Guest[a]

			caps		
guest	volume ($Å^3$)	polar surface area ($Å^2$)	CsCs	RbRb	KK
CH_3Cl	47.2	0	2.50 ± 0.14	1.84 ± 0.47	2.33 ± 0.16
HCN	35.2	15.3	1.98 ± 0.02	1.82 ± 0.02	2.21 ± 0.04
CH_3CN	53.1	15.3	0.63 ± 0.01		
CH_3OH	40.5	20.4	1.59 ± 0.01	1.81 ± 0.00	1.61 ± 0.01
CO_2	38.4	28.9	0.91 ± 0.03	1.03 ± 0.05	0.97 ± 0.00
HCOOH	43.0	34.7	0.80 ± 0.00	0.86 ± 0.04	0.96 ± 0.02
NH_3	22.8	41.5	0.42 ± 0.00	0.99 ± 0.02	0.80 ± 0.01

[a]A standard deviation of 0.00 is reported for standard deviation of less than 0.005 determined from three or more replicate measurements.

DOI: 10.1021/acs.jpca.8b08031
J. Phys. Chem. A 2018, 122, 9224−9232

(when the metal ion is not lost, the experiment gives no means of distinguishing which portal was used).

CONCLUSIONS

The loss of guests from mc5 complexes with two alkali metal ion caps is investigated using collision-induced dissociation techniques and molecular mechanics simulations. Similar results are generally obtained using both methods, indicating that molecular mechanics simulations using the MMFF94 force field can be used to approximate the relative stability of mc5 molecular container complexes and likely the stability of other similar complexes. For guests that *do not have* polar bonds, the extrusion barrier increases with increasing guest volume, likely because larger guests require more displacement of the metal ion caps to egress from the complexes than smaller guests. The extrusion barriers of guests that *have* polar bonds are lower than those of guests of similar size that *do not have* polar bonds, and a decrease in the extrusion barrier is observed for guests that have polar bonds as the polar surface area of the guest increases. This is likely because electrostatic interactions between the partial charges on the guests and the ion caps and rim oxygens of mc5 stabilize the dissociation intermediates of these complexes, with higher polar surface areas resulting in more stable intermediates. The nature of the ion caps appears to have little effect on the dissociation threshold for loss of a guest except in extreme conditions, such as for relatively large guests that sterically displace the ion caps and guests with relatively high polar surface areas that form more stable dissociation intermediates with the larger caps than with the smaller caps. Results from this study demonstrate that the size and shape of a guest and the ability of the guest to interact with the portals and capping agents of a molecular container all contribute to the stability of a molecular container complex. Initial results obtained for other cucurbit[5]uril derivatives appear to follow similar trends as those reported here for mc5. However, additional experiments are still needed to determine the effects of the rigidity, cavity size, and portal width of cucurbituril-based molecular containers on the extrusion barrier for loss of a guest.

AUTHOR INFORMATION

Corresponding Author

*Phone (801) 422-2355; e-mail david_dearden@byu.edu.

ORCID

David V. Dearden: 0000-0003-0899-7776

Notes

The authors declare no competing financial interest.

ACKNOWLEDGMENTS

The authors thank IBC Advanced Technologies (American Fork, UT) for supplying samples of mc5 and the National Science Foundation for funding (CHE-1412289).

REFERENCES

(1) Ruhle, B.; Saint-Cricq, P.; Zink, J. I. Externally Controlled Nanomachines on Mesoporous Silica Nanoparticles for Biomedical Applications. *ChemPhysChem* **2016**, *17*, 1769−1779.

(2) Cram, D. J. Molecular Container Compounds. *Nature* **1992**, *356*, 29−36.

(3) Mal, P.; Breiner, B.; Rissanen, K.; Nitschke, J. R. White Phosphorus Is Air-Stable Within a Self-Assembled Tetrahedral Capsule. *Science* **2009**, *324*, 1697−1699.

(4) Gibb, C. L. D.; Sundaresan, A. K.; Ramamurthy, V.; Gibb, B. C. Templation of the Excited-state Chemistry of α-(n-Alkyl) Dibenzyl Ketones: How Guest Packing Within a Nanoscale Supramolecular Capsule Influences Photochemistry. *J. Am. Chem. Soc.* **2008**, *130*, 4069−4080.

(5) Lee, T. C.; Kalenius, E.; Lazar, A. I.; Assaf, K. I.; Kuhnert, N.; Grun, C. H.; Janis, J.; Scherman, O. A.; Nau, W. M. Chemistry Inside Molecular Containers in the Gas Phase. *Nat. Chem.* **2013**, *5*, 376−382.

(6) Steed, J. W.; Atwood, J. L. *Supramolecular Chemistry*, 2nd ed.; Wiley: Chichester, UK, 2009.

(7) Mitkina, T.; Fedin, V.; Llusar, R.; Sorribes, I.; Vicent, C. Distinctive Unimolecular Gas-phase Reactivity of $[M(En)_2]^{2+}$ (M = Ni, Cu) Dications and Their Inclusion Complexes with the Macrocyclic Cavitand Cucurbit[8]uril. *J. Am. Soc. Mass Spectrom.* **2007**, *18*, 1863−1872.

(8) Dearden, D. V.; Ferrell, T. A.; Asplund, M. C.; Zilch, L. W.; Julian, R. R.; Jarrold, M. F. One Ring to Bind Them All: Shape-Selective Complexation of Phenylenediamine Isomers with Cucurbit[6]uril in the Gas Phase. *J. Phys. Chem. A* **2009**, *113*, 989−997.

(9) Zhang, H.; Grabenauer, M.; Bowers, M. T.; Dearden, D. V. Supramolecular Modification of Ion Chemistry: Modulation of Peptide Charge State and Dissociation Behavior through Complexation with Cucurbit[n]uril (n = 5, 6) or α-Cyclodextrin. *J. Phys. Chem. A* **2009**, *113*, 1508−1517.

(10) Deroo, S.; Rauwald, U.; Robinson, C. V.; Scherman, O. A. Discrete, Multi-component Complexes With Cucurbit[8]Uril in the Gas-Phase. *Chem. Commun.* **2009**, 644−646.

(11) Noh, D. H.; Lee, S. J. C.; Lee, J. W.; Kim, H. I. Host-Guest Chemistry in the Gas Phase: Complex Formation of Cucurbit[6]uril with Proton-bound Water Dimer. *J. Am. Soc. Mass Spectrom.* **2014**, *25*, 410−421.

(12) Lagona, J.; Mukhopadhyay, P.; Chakrabarti, S.; Isaacs, L. The Cucurbit[n]uril Family. *Angew. Chem., Int. Ed.* **2005**, *44*, 4844−4870.

(13) Freeman, W. A.; Mock, W. L.; Shih, N. Y. Cucurbituril. *J. Am. Chem. Soc.* **1981**, *103*, 7367−7368.

(14) Assaf, K. I.; Nau, W. M. Cucurbiturils: from Synthesis to High-Affinity Binding and Catalysis. *Chem. Soc. Rev.* **2015**, *44*, 394−418.

(15) Cong, H.; Ni, X. L.; Xiao, X.; Huang, Y.; Zhu, Q. J.; Xue, S. F.; Tao, Z.; Lindoy, L. F.; Wei, G. Synthesis and Separation of Cucurbit[n]urils and Their Derivatives. *Org. Biomol. Chem.* **2016**, *14*, 4335−4364.

(16) Mock, W. L.; Shih, N. Y. Host Guest Binding-Capacity Of Cucurbituril. *J. Org. Chem.* **1983**, *48*, 3618−3619.

(17) Nau, W. M.; Florea, M.; Assaf, K. I. Deep Inside Cucurbiturils: Physical Properties and Volumes of their Inner Cavity Determine the Hydrophobic Driving Force for Host-Guest Complexation. *Isr. J. Chem.* **2011**, *51*, 559−577.

(18) Rekharsky, M. V.; Mori, T.; Yang, C.; Ko, Y. H.; Selvapalam, N.; Kim, H.; Sobransingh, D.; Kaifer, A. E.; Liu, S. M.; Isaacs, L.; et al. A Synthetic Host-guest System Achieves Avidin-Biotin Affinity by Overcoming Enthalpy-Entropy Compensation. *Proc. Natl. Acad. Sci. U. S. A.* **2007**, *104*, 20737−20742.

(19) Barrow, S. J.; Kasera, S.; Rowland, M. J.; del Barrio, J.; Scherman, O. A. Cucurbituril-based Molecular Recognition. *Chem. Rev.* **2015**, *115*, 12320−12406.

(20) Kellersberger, K. A.; Anderson, J. D.; Ward, S. M.; Krakowiak, K. E.; Dearden, D. V. Encapsulation of N_2, O_2, Methanol, or Acetonitrile by dDcamethylcucurbit[5]uril$(NH_4^+)_2$ Complexes in the Gas Phase: Influence of the Guest on "Lid" Tightness. *J. Am. Chem. Soc.* **2001**, *123*, 11316−11317.

(21) Jeon, Y. J.; Kim, H.; Jon, S.; Selvapalam, N.; Oh, D. H.; Seo, I.; Park, C. S.; Jung, S. R.; Koh, D. S.; Kim, K. Artificial Ion Channel Formed by Cucurbit[N]uril Derivatives with a Carbonyl Group Fringed Portal Reminiscent of the Selectivity Filter of K^+ Channels. *J. Am. Chem. Soc.* **2004**, *126*, 15944−15945.

(22) Choi, J.; Kim, J.; Kim, K.; Yang, S. T.; Kim, J. I.; Jon, S. A Rationally Designed Macrocyclic Cavitand that Kills Bacteria with

DOI: 10.1021/acs.jpca.8b08031
J. Phys. Chem. A 2018, 122, 9224−9232

High Efficacy and Good Selectivity. *Chem. Commun.* **2007**, 1151−1153.
(23) Montes-Navajas, P.; Gonzalez-Bejar, M.; Scaiano, J. C.; Garcia, H. Cucurbituril Complexes Cross the Cell Membrane. *Photochem. Photobiol. Sci.* **2009**, *8*, 1743−1747.
(24) Dong, N.; Xue, S. F.; Zhu, Q. J.; Tao, Z.; Zhao, Y.; Yang, L. X. Cucurbit[n]urils (n = 7, 8) Binding of Camptothecin and the Effects on Solubility and Reactivity of the Anticancer Drug. *Supramol. Chem.* **2008**, *20*, 663−671.
(25) Park, K. M.; Suh, K.; Jung, H.; Lee, D. W.; Ahn, Y.; Kim, J.; Baek, K.; Kim, K. Cucurbituril-based Nanoparticles: a New Efficient Vehicle for Targeted Intracellular Delivery of Hydrophobic Drugs. *Chem. Commun.* **2009**, 71−73.
(26) Hettiarachchi, G.; Nguyen, D.; Wu, J.; Lucas, D.; Ma, D.; Isaacs, L.; Briken, V. Toxicology and Drug Delivery by Cucurbit[n]-uril Type Molecular Containers. *PLoS One* **2010**, *5*, No. e10514.
(27) Wheate, N. J.; Limantoro, C. Cucurbit[n]urils as Excipients in Pharmaceutical Dosage Forms. *Supramol. Chem.* **2016**, *28*, 849−856.
(28) Nguyen, H. D.; Dang, D. T.; van Dongen, J. L. J.; Brunsveld, L. Protein Dimerization Induced by Supramolecular Interactions with Cucurbit[8]uril. *Angew. Chem., Int. Ed.* **2010**, *49*, 895−898.
(29) Lee, H. H. L.; Heo, C. E.; Seo, N.; Yun, S. G.; An, H. J.; Kim, H. I. Accurate Quantification of N-Glycolylneuraminic Acid in Therapeutic Proteins Using Supramolecular Mass Spectrometry. *J. Am. Chem. Soc.* **2018**, DOI: 10.1021/jacs.8b07864.
(30) Cong, H.; Zhao, F. F.; Zhang, J. X.; Zeng, X.; Tao, Z.; Xue, S. F.; Zhu, Q. J. Rapid Transformation of Benzylic Alcohols to Aldehyde in the Presence of Cucurbit[8]uril. *Catal. Commun.* **2009**, *11*, 167−170.
(31) Wang, Y. H.; Cong, H.; Zhao, F. F.; Xue, S. F.; Tao, Z.; Zhu, Q. J.; Wei, G. Selective Catalysis for the Oxidation of Alcohols to Aldehydes in the Presence of Cucurbit[8]uril. *Catal. Commun.* **2011**, *12*, 1127−1130.
(32) Basilio, N.; Garcia-Rio, L.; Moreira, J. A.; Pessego, M. Supramolecular Catalysis by Cucurbit[7]uril and Cyclodextrins: Similarity and Differences. *J. Org. Chem.* **2010**, *75*, 848−855.
(33) Mock, W. L.; Irra, T. A.; Wepsiec, J. P.; Manimaran, T. L. Cycloaddition Induced By Cucurbituril - A Case Of Pauling Principle Catalysis. *J. Org. Chem.* **1983**, *48*, 3619−3620.
(34) Buschmann, H. J.; Schollmeyer, E. Cucurbituril and β-Cyclodextrin as Hosts for the Complexation of Organic Dyes. *J. Inclusion Phenom. Mol. Recognit. Chem.* **1997**, *29*, 167−174.
(35) Dsouza, R. N.; Pischel, U.; Nau, W. M. Fluorescent Dyes and Their Supramolecular Host/Guest Complexes with Macrocycles in Aqueous Solution. *Chem. Rev.* **2011**, *111*, 7941−7980.
(36) Cong, H.; Li, C. R.; Xue, S. F.; Tao, Z.; Zhu, Q. J.; Wei, G. Cucurbituril-resisted Acylation of the anti-Tuberculosis Drug Isoniazid via a Supramolecular Strategy. *Org. Biomol. Chem.* **2011**, *9*, 1041−1046.
(37) Masson, E.; Ling, X. X.; Joseph, R.; Kyeremeh-Mensah, L.; Lu, X. Y. Cucurbituril Chemistry: a Tale of Supramolecular Success. *RSC Adv.* **2012**, *2*, 1213−1247.
(38) Zhang, X. X.; Krakowiak, K. E.; Xue, G. P.; Bradshaw, J. S.; Izatt, R. M. A Highly Selective Compound for Lead: Complexation Studies of Decamethylcucurbit[5]uril with Metal Ions. *Ind. Eng. Chem. Res.* **2000**, *39*, 3516−3520.
(39) Mortensen, D. N.; Dearden, D. V. Influence of Charge Repulsion on Binding Strengths: Experimental and Computational Characterization of Mixed Alkali Metal Complexes of Decamethylcucurbit[5]uril in the Gas Phase. *Chem. Commun.* **2011**, *47*, 6081−6083.
(40) Strohalm, M.; Hassman, M.; Košata, B.; Kodíček, M. mMass Data Miner: an Open Source Alternative for Mass Spectrometric Data Analysis. *Rapid Commun. Mass Spectrom.* **2008**, *22*, 905−908.
(41) Blakney, G. T.; Hendrickson, C. L.; Marshall, A. G. Predator Data Station: a Fast Data Acquisition System for Advanced FT-ICR MS Experiments. *Int. J. Mass Spectrom.* **2011**, *306*, 246−252.
(42) Wigger, M.; Nawrocki, J. P.; Watson, C. H.; Eyler, J. R.; Benner, S. A. Assessing Enzyme Substrate Specificity Using Combinatorial Libraries and Electrospray Ionization Fourier Transform Ion Cyclotron Resonance Mass Spectrometry. *Rapid Commun. Mass Spectrom.* **1997**, *11*, 1749−1752.
(43) Chen, L.; Wang, T. C. L.; Ricca, T. L.; Marshall, A. G. Phase-Modulated Stored Wave-Form Inverse Fourier-Transform Excitation for Trapped Ion Mass-Spectrometry. *Anal. Chem.* **1987**, *59*, 449−454.
(44) Gauthier, J. W.; Trautman, T. R.; Jacobson, D. B. Sustained Off-Resonance Irradiation For Collision-Activated Dissociation Involving Fourier-Transform Mass-Spectrometry - Collision-Activated Dissociation Technique That Emulates Infrared Multiphoton Dissociation. *Anal. Chim. Acta* **1991**, *246*, 211−225.
(45) Jiao, C. Q.; Ranatunga, D. R. A.; Vaughn, W. E.; Freiser, B. S. A Pulsed-Leak Valve for Use with Ion Trapping Mass Spectrometers. *J. Am. Soc. Mass Spectrom.* **1996**, *7*, 118−122.
(46) Zhang, H. Z.; Ferrell, T. A.; Asplund, M. C.; Dearden, D. V. Molecular Beads on a Charged Molecular String: α,ω-Alkyldiammonium Complexes of Cucurbit[6]uril in the Gas Phase. *Int. J. Mass Spectrom.* **2007**, *265*, 187−196.
(47) Halgren, T. A. Merck Molecular Force Field. I. Basis, Form, Scope, Parameterization, and Performance of MMFF94. *J. Comput. Chem.* **1996**, *17*, 490−519.
(48) Halgren, T. A. Merck Molecular Force Field. II. MMFF94 van der Waals and Electrostatic Parameters for Intermolecular Interactions. *J. Comput. Chem.* **1996**, *17*, 520−552.
(49) Halgren, T. A. Merck Molecular Force Field. III. Molecular Geometries and Vibrational Frequencies for MMFF94. *J. Comput. Chem.* **1996**, *17*, 553−586.
(50) Halgren, T. A.; Nachbar, R. B. Merck Molecular Force Field. IV. Conformational Energies and Geometries for MMFF94. *J. Comput. Chem.* **1996**, *17*, 587−615.
(51) Halgren, T. A. Merck Molecular Force Field. V. Extension of MMFF94 using Experimental Data, Additional Computational Data, and Empirical Rules. *J. Comput. Chem.* **1996**, *17*, 616−641.
(52) Bondi, A. van der Waals Volumes and Radii. *J. Phys. Chem.* **1964**, *68*, 441−451.
(53) Ertl, P. Molecular Drug Properties: Measurement and Prediction. In *Polar Surface Area*; Mannhold, R., Kubinyi, H., Folkers, G., Eds.; Wiley-VCH: Weinheim, Germany, 2007; Vol. *37*, pp 111−126.
(54) Marquez, C.; Nau, W. M. Two Mechanisms of Slow Host-Guest Complexation between Cucurbit[6]uril and Cyclohexylmethylamine: pH-Responsive Supramolecular Kinetics. *Angew. Chem., Int. Ed.* **2001**, *40*, 3155−3160.
(55) Flinn, A.; Hough, G. C.; Stoddart, J. F.; Williams, D. J. Decamethylcucurbit[5]uril. *Angew. Chem., Int. Ed. Engl.* **1992**, *31*, 1475−1477.

DOI: 10.1021/acs.jpca.8b08031
J. Phys. Chem. A 2018, 122, 9224−9232